The Effects of Ground Permittivity and Surface Roughness on Multi-Path Measurements at K-band

Joseph D. Brunett*, Farshid Aryanfar, Kamran Entesari, and Taesik Yang
jbrunett@umich.edu, faryanfa@umich.edu, kentesar@umich.edu, taesiky@umich.edu
Radiation Laboratory, EECS Department
The University of Michigan

I. Introduction

In the past decade a number of automotive radar systems have been designed with application to adaptive cruise control, road surface monitoring, accurate speed measurement, and potential application to collision avoidance. In order to construct these high-tech radar systems for the automotive market, a thorough understanding of the residential and highway environments in which they would operate is required. In this paper, a versatile open-ended waveguide measurement technique [1] is used to determine the effective dielectric permittivity of various ground types. From this information, K-band LOS (Line-Of-Sight) propagation above different ground materials are calculated and compared with outdoor measurements. Here the influence of ground permittivity, surface roughness, and ground layer thickness on K-band propagation is presented.

II. Complex Permittivity of the Ground

Numerous techniques have been developed and tested for dielectric constant measurement [2]. The most common methods include: partially or fully filled transmission lines and cavities, open-ended transmission lines and waveguides, free-space reflection and transmission, and inverse scattering [2]. Because our focus in this paper emphasizes inhomogeneous materials with varying levels of water content, a cavity or transmission line filled dielectric measurement apparatus is not practical. Similarly, an inverse scattering method would require a complete coherent K-band radar system, something not readily available. Hence, for this study we have selected an open-ended transmission line method.

The open-ended waveguide method [1] is quite suitable for general lossy dielectric materials (or materials of infinite extent) and requires no significant material preparation. In this method, the conductance (G) and susceptance (B) of the aperture radiating into the dielectric half space is obtained by measuring the reflection coefficient from the waveguide probe that is in contact with the dielectric sample. Given G and B, the dielectric constant is determined using an integral equation. As it is shown in Figure 1 [1], the imaginary part of the effective dielectric constant (ε_r'') is nearly insensitive to G and therefore the real part of the effective dielectric constant (ε_r') can be closely approximated independent of ε_r''. Using ε_r', the imaginary component of the dielectric constant (ε_r'') is derived from B. Finally, using these initial values of the permitivity; the same process is iterated to determine the permittivity values to within a given tolerance.

0-7803-7846-6/03/$17.00 ©2003 IEEE

For the ground samples shown in Figure 2, five independent reflection coefficient measurements were taken. From these the dielectric constants were obtained and are listed in Table 1. The measured reflection coefficients over the five trials show slight amplitude and phase variation. If we assume this is entirely due to changes in the material permittivity at different positions, then we can find a reasonable permittivity for the sample based on the average of the permittivities over the five samples. However, if some of this variation is due to errors in measurement procedure, then the average of the values for Γ should be computed, and permittivity should be derived from that value. The results for both scenarios are listed in Table 1.

Table 1. Dielectric Permittivity of Ground Materials

Material	$\bar{\varepsilon}_r'$	$\bar{\varepsilon}_r''$	$\varepsilon_r'(\Gamma_{av})$	$\varepsilon_r''(\Gamma_{av})$	Material	$\bar{\varepsilon}_r'$	$\bar{\varepsilon}_r''$	$\varepsilon_r'(\Gamma_{av})$	$\varepsilon_r''(\Gamma_{av})$
Sand	3.72	3.33	3.65	3.36	Wet Grass	18.16	2.19	18.28	2.20
Dry Grass	3.39	1.66	3.51	1.64	Teflon**	1.81	0.009	-	-
Road Fill	16.55	3.83	16.44	3.83	Asphalt*	3.18	0.04	-	-

Note*: The asphalt layer thickness (2 cm) was not sufficient to be assumed as an infinite half space. Therefore the method stated in this paper cannot be applied. The data for the asphalt in table (1) and simulation are based on [2]. ** Teflon was used for calibration.

III. Antenna Calibration for LOS Measurement

In order to make accurate comparisons between measurement and theoretical results it was necessary to characterize the gain and pattern of the transmitting and receiving antennas. The receiving antenna is a standard-gain horn and its parameters are known. Far field pattern and gain measurements for the transmitting antenna were made to determine its characteristics. Also, as a second approach, a planar near field antenna measurement setup [3] was used to calculate the directivity of the transmitting antenna based on the antenna's total pattern.

The far field power pattern of the transmitting antenna is plotted in Figure 3. Using the Friis equation and the data in Figure 3, the reflector gain, directivity, HPBW and efficiency are computed and summarized in Table 2. In calculating the maximum directivity of the dish antenna, the equations (1) and (2) are compared.

$$D_0 \cong \frac{72815}{\Theta_{1d}^2 + \Theta_{2d}^2} \tag{1}$$

where θ_{1d} and θ_{2d} are the HPBW (in degrees) in the E and H plane respectively. In (2), the total far field power pattern is integrated from the near field transformed data. The integration method is used to calculate the beam solid angle by integrating over the normalized 3D power pattern, as obtained here from the transformed near field measurement. In practice, this integral was converted to a summation of discrete values of θ and ϕ [4].

$$D_0 = \frac{4\pi}{\Omega_A} = \frac{4\pi}{\int_{\phi=0}^{2\pi}\int_{\theta=0}^{\pi} F_n(\theta,\psi)\sin(\theta)\cdot d\theta\cdot d\phi} \cong \frac{4\pi}{\left(\frac{\pi}{N}\right)\left(\frac{2\pi}{M}\right)\sum_{j=1}^{M}\left[\sum_{i=1}^{N} F_n(\theta_i,\psi_j)\sin(\theta_i)\right]} \tag{2}$$

For the near field measurement, the dimensions of the scanning area and probe distance from aperture were calculated to ensure accurate characterization of the

far field pattern; spatial sampling was maintained at less than $\lambda_o/2$ to prevent aliasing. Table 2 also summarizes the antenna characteristics as derived from the transformed near field data.

Table 2. Transmitting and Receiving Antenna Characteristics

Characteristic	FF data	NF Transformed Data	Standard Gain Horn
HPBW	E 3.0° / H 3.6°	E 2.8° / H 3.6°	E 8.2° / H 9.8°
Directivity	35.44 dB	35.8 dB	27.1 dB
Gain	34.78 dB	34.78 dB (from FF)	24.52 dB
Efficiency	86 %	79 %	55%

IV. Multi-Path Measurements

Using the setup shown in the Figure 4, two LOS measurements were performed: one above a smooth asphalt road ($\sigma_o \approx 3$mm) and the other above a rough grass field ($\sigma_o \approx 2$cm). Figures 5 and 6 show the measured and theoretical interference patterns that result. Assuming the ground is a homogeneous half space, received power is calculated by Friis formula, including the contribution from the reflected path (3).

$$P_r = P_t G_t(\theta,\psi) G_r(\theta,\psi) \left(\frac{\lambda}{4\pi}\right)^2 \left| \frac{1}{D} + \frac{\tilde{\Gamma}}{R} e^{-jk(R-D)} \right|^2 \tag{3}$$

However, as we see in Figure 5, the theoretical result does not match the measurement data above the road. This error is directly attributed to the multi-layer structure of the road surface. If we consider the roadway as a two-layered medium, Γ is modified to (4) with the first layer being asphalt and the second layer being road fill.

$$\Gamma = \frac{\Gamma_{12} + \Gamma_{23} e^{-j2k_2 h \cos\theta_2}}{1 + \Gamma_{12}\Gamma_{23} e^{-j2k_2 h \cos\theta_2}} \tag{4}$$

In (4), Γ_{ij} is the reflection coefficient between layers i and j and h is the first layer thickness. In Figure 6, the theoretical interference pattern (based on the measured dielectric permittivity of the wet and dry grass) does not match perfectly with the measured data. The magnitude of the signal is similar, but the predictable interference pattern is inhibited by the random scattering of the rough grass surface.

V. Conclusions

Using an open-ended waveguide dielectric measurement technique on different ground materials, a multi-layer ground model has been developed. The model has been used in path loss calculation and shows a good agreement with measurement results (±1 dB for road and ±2 dB for grass). These measurements demonstrate that for the rough surfaces, a more advance model is required for accurate propagation modeling.

References

[1] S. Ganchev, R. Zoughi, "A Novel Technique for Dielectric Measurement of Generally Lossy Dielectrics," *IEEE Trans. Inst. and Meas.*, Vol. 41, No. 3, June 1992.

[2] K. Sarabandi, E. S. Li, A. Nashashibi,"Modeling and Measurements of Scattering from Road Surfaces at Millimeter-Wave Frequencies," *IEEE Trans. Antennas Propag.*, Vol. 45, Nov. 1997.
[3] D. Zahn and K. Sarabandi, "Near field measurements of bistatic scattering from random rough surfaces," IEEE Ant. and Propag. Society Int. Symposium, Vol. 3, pp.1730 –1733, 2000.
[4] C. A. Balanis, "Antenna Theory, Analysis and Design," *John Wiely and Sons Inc.*, 1997.

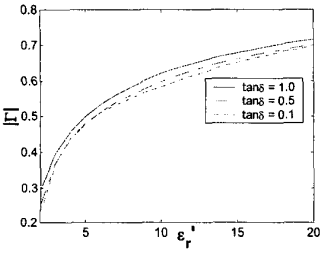

Figure 1. Magnitude of Reflection Coefficient is insensitive to imaginary part of dielectric constant [1]

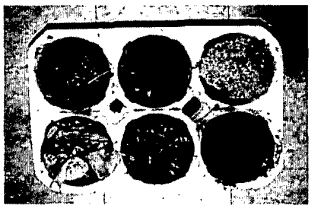

Figure 2. Samples of ground materials

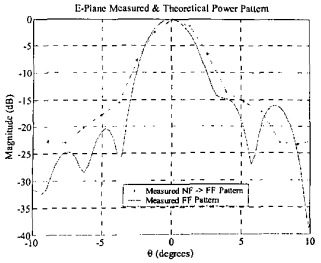

Figure 3. TX Antenna Power Pattern

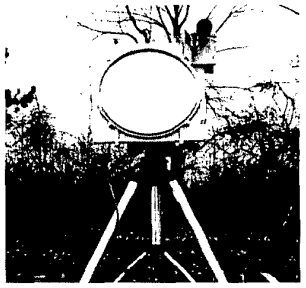

Figure 4. Transmitter setup with aligner

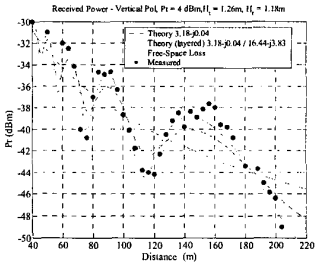

Figure 5. LOS Propagation above Roadway

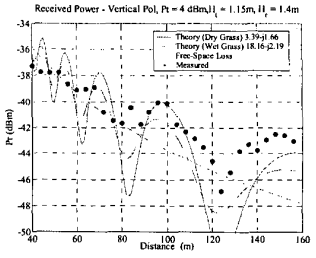

Figure 6. LOS Propagation above Field